Spatial and Temporal Influence of Sea Level on Inland Stress based on Seismic Velocity Monitoring

Rezkia Dewi Andajani (rezkiadewiandajani90@mine.kyushu-u.ac.jp)
Kyushu University https://orcid.org/0000-0003-3926-2633
Takeshi Tsuji
Kyushu University - Ito Campus: Kyushu Daigaku
Roel Snieder
Colorado School of Mines
Tatsunori Ikeda
Kyushu University: Kyushu Daigaku

Full paper

Keywords: seismic velocity change, sea level change, ocean loading, inland deformation

Posted Date: May 7th, 2021

DOI: https://doi.org/10.21203/rs.3.rs-489282/v1

Spatial and temporal influence of sea level on inland stress based on seismic velocity monitoring

Rezkia Dewi Andajani[1*]

[1]Department of Earth Resources Engineering, Kyushu University, 744 Motooka, Nishi-ku, Fukuoka 819-0395, Japan (Email: rezkiadewiandajani90@mine.kyushu-u.ac.jp).

Takeshi Tsuji[1,2,3]

[1]Department of Earth Resources Engineering, Kyushu University, 744 Motooka, Nishi-ku, Fukuoka 819-0395, Japan. [2] International Institute for Carbon-Neutral Energy Research (WPI-I2CNER), Kyushu University, 744 Motooka, Nishi-ku, Fukuoka 819-0395, Japan. [3]Disaster Prevention Research Institute, Kyoto University Gokasho, Uji, Kyoto 611-0011, Japan (Email: tsuji@mine.kyushu-u.ac.jp).

Roel Snieder[4]

[4]Colorado School of Mines, Golden CO 80401-1887, USA. (Email: rsnieder@mines.edu)

Tatsunori Ikeda[1,2]

[1]Department of Earth Resources Engineering, Kyushu University, 744 Motooka, Nishi-ku, Fukuoka 819-0395, Japan. [2]International Institute for Carbon-Neutral Energy Research (WPI-I2CNER), Kyushu University, 744 Motooka, Nishi-ku, Fukuoka 819-0395, Japan (Email: ikeda@mine.kyushu-u.ac.jp).

*Corresponding author: Rezkia Dewi Andajani (rezkiadewiandajani90@mine.kyushu-u.ac.jp)

Abstract

Earth's crust responds to perturbations from various environmental factors. To evaluate this response, seismic velocity changes offer an indirect diagnostic, especially where velocity can be monitored on an ongoing basis from ambient seismic noise. Investigating the connection between the seismic velocity changes and external perturbations could be useful for characterizing dynamic activities in the crust. The seismic velocity is known to be sensitive to variations in meteorological signals such as temperature, snow, and precipitation as well as changes in sea level. Among these perturbations, the impact of variations in sea level on velocity changes inferred from seismic interferometry of ambient noise is not well known. This study investigates the influence of the ocean in a 3-year record of ambient noise seismic velocity monitoring in the Chugoku and Shikoku regions of southwest Japan. First, we applied a bandpass filter to determine the optimal period band for discriminating among different influences on seismic velocity. Then, we applied a regression analysis between the proximity of seismic station pairs to the coast and the ocean influence, as indicated by the correlation of sea level to seismic velocity changes between pairs of stations. Our study suggests that for periods between 0.0036 to 0.01 cycle/day (100–274 days), the ocean's influence on seismic velocity decreases with increasing distance of station pairs from the coast. The increasing sea level deforms the ocean floor, affecting the stress in the adjacent coast. The stress change induced by the ocean loading may extend at least dozens of kilometers from the coast. The correlation between sea level and inland seismic velocity changes are negative or positive. Although it is difficult to clearly interpret the correlation based on simple

model, they could depend on the in situ local stress, orientation of dominant crack, and hydraulic conductivity. Our study shows that seismic monitoring may be useful for evaluating the perturbation in the crust associated with an external load.

Keywords: seismic velocity change, sea level change, ocean loading, inland deformation

Introduction

The understanding of how the Earth's crust responds to various environmental perturbations is important for earthquake evaluations, geological storage facilities, and geothermal developments. Temporal variations in seismic velocity can be linked to the activities of volcanoes and earthquakes (e.g., Hutapea et al. 2020; Nimiya et al. 2017; Rivet et al. 2014; Takano et al. 2017). They are also sensitive to surface perturbations associated with climatic perturbations such as rainfall (Nakata and Snieder 2012; Sens-Schönfelder and Wegler 2006; Andajani et al. 2020), snow (Mordret et al. 2016), atmospheric pressure (Niu et al. 2008; Silver et al. 2007), and temperature (Hillers et al. 2015; Richter et al. 2014).

The influence of environmental perturbations on seismic velocity changes can be presumed to differ for various locations. For example, since volcanic regions are sensitive to internal and external forcing (e.g., Albino et al. 2010; Matthews et al. 2009; Neuberg 2000), seismic velocity changes in volcanic regions should be analyzed in terms of surface perturbations as well as magmatic and tectonic activities (e.g., Donaldson et

al. 2019). Precipitation dominates the temporal seismic velocity changes in locations where groundwater is rapidly recharged (e.g., Andajani et al. 2020; Sens-Schönfelder and Wegler 2006). In arid regions, temperature is likely to dominate the variations of seismic velocity (Hillers et al. 2015). The influence of atmospheric pressure is likely to apply to any location, and its effect is observable as deep as seismogenic depths (Niu et al. 2008).

A previous study has shown that precipitation, snow, and sea level influence the crustal deformation of the Japan Islands as detected by ambient noise correlation (Wang et al. 2017). It is less well known how changes in sea level, such as its current global rise, affect seismic velocity changes. The crust of Japan is known to be affected by the loading from the ocean (Hatanaka et al. 2001; Sato et al. 2001); thus, we sought in this study to better characterize the effect of sea level variations on estimated seismic velocity changes by considering its spatial variation.

This work is a continuation of our research that has been interpreting seismic velocity changes from ambient noise in the Chugoku and Shikoku regions of southwest Japan (Andajani et al. 2020). The study region is surrounded by the Seto inland sea, Japan sea, and the Pacific coast. This region lacks active volcanoes and is subject to heavy rain, where water can be directly discharged to the coast by rivers if there is no rainfall infiltration. Snow is uncommon and its influence is assumed to be negligible.

The influence of the ocean should be strongest in the coastal environment and should decrease with increasing distance to the ocean. In this study, we seek to estimate the spatial scale of this effect by searching for the period band where the relationship

between sea level variability and seismic velocity changes can best be identified. We find that in the period band, from 100 to 274 days (0.0036 – 0.01 cycle/day), the influence of sea level on seismic velocity change tends to decrease with the increasing station's distance from the coast. We interpret this result as inland stress changes induced by ocean loading.

Data preparation

We used seismic data for 99 Hi-net seismic stations in Chugoku and Shikoku (Fig. 1) from the National Research Institute for Earth Science and Disaster Resilience (NIED) (Obara et al. 2005). The Chugoku region is composed chiefly of volcanic and granitic rocks, whereas Shikoku Island consists mostly of the Sanbagawa metamorphic belt and multiple accretionary complexes (Fig. 1b). Using seismic velocity changes estimated from ambient noise for 306 station pairs, we compared the time series of seismic velocity change to meteorological data for the same region during the years 2015–2017. We used sea level and atmospheric pressure data recorded by the Japan Meteorological Agency (JMA) along the Chugoku and Shikoku coasts (Figs. 1d and 1e).

Our study utilized seismic velocity changes inferred from the coda of the cross correlation of the recorded vertical component (see Andajani et al. 2020 and Hutapea et al. 2020 for details). The time window of 100 s of the coda wave was selected to estimate the seismic velocity changes by stretching interpolation method (Hadziioannou et al. 2009; Hutapea et al. 2020; Minato et al. 2012; Nimiya et al. 2017) where one maximizes:

$$CC(\varepsilon) = \frac{\int f_\varepsilon^{cur}(t) f^{ref}(t) dt}{(\int (f_\varepsilon^{cur}(t))^2 dt \int (f^{ref}(t))^2 dt)^{1/2}}, \quad (1)$$

with

$$f_\varepsilon^{cur}(t) = f^{cur}\big(t(1+\varepsilon)\big), \quad (2)$$

where f^{ref} represents the reference trace, f^{cur} is the current trace, and t is time. The stretching interpolation method elongates the time axis and searches for traces similar to the reference trace based on the correlation coefficient $CC(\varepsilon)$. In our analysis of the 3-year dataset of seismic velocity change data, we analyzed the seismic velocity change on each year individually by using the sliding reference method (SRM) (Hutapea et al. 2020). We defined the reference trace f^{ref} as the 1-year stack of coda of cross-correlation data and used the 10-day stack of coda of cross-correlation as the current trace f^{cur}. The stretching parameter ε is related to the relative time shift ($\Delta t/t$) and the velocity change ($\Delta v/v$) described in

$$\varepsilon = \Delta t/t = -(\Delta v/v). \quad (3)$$

The average stretching correlation coefficients for all estimated seismic station pairs are shown in Figure S1 of the additional file 1. The lowest stretching correlation coefficient is ~0.5. Most of the station pairs (210 of 306) have stretching correlation coefficients greater than 0.6, meaning that the estimated seismic velocity changes in the Chugoku and Shikoku regions are stable.

The observed sea level is a composite of geophysical cycles that include tidal variations (astronomical tides), non-tidal variations (meteorological contributions), and mean sea levels (Haigh 2017). We computed our time series of daily sea level by averaging 24 hours of data (Additional file 1: Fig. S2a). Averaging the hourly sea level over each day tends to suppress semidiurnal and diurnal variations, although longer period variations such as the fortnightly lunar or semiannual solar cycle may remain. Because the amplitudes of these long-period cycles of the astronomical tide are small, sea level variation is usually dominated by the non-tidal processes (Woodworth et al. 2019). Thus, we took the dominance of non-tidal processes in sea level variability as an assumption. As for the atmospheric pressure, we directly collected the data from JMA.

Methods

Our investigation of the influence of sea level changes on seismic velocity changes comprised three steps (Fig. 2). The first step was to distinguish the respective cycles of sea level and atmospheric pressure. Sea level and atmospheric pressure tend to have dominant cycles that are similar, as indicated by Pearson correlation coefficients as great as –0.68 (Additional file 1: Fig. S2). The correlation between these two-time series would raise a difficulty in unraveling the contribution of sea level and atmospheric pressure on seismic velocity. Therefore, we searched for the optimum period bands in the dataset to distinguish the two cycles. Once the best period band was identified, in step 2 we estimated the influence of sea level on seismic velocity by calculating the Pearson correlation coefficient of the two time series after filtering by that period band.

Correlation coefficients were calculated for each seismic station pair. Finally, in step 3, we evaluated the relationship between correlation coefficients and the proximity of seismic stations to the coast. Considering that the ocean caused perturbations on the seabed and the nearby shore, we searched for the possibility of decreasing correlations obtained from step 2 with increasing distance from the ocean. Assuming a linear relationship, we used a statistical approach to evaluate the evidence of decreasing correlations with increasing distance from the coast.

Step 1: Distinguishing cycles of sea level and atmospheric pressure

Atmospheric pressure loading can cause crustal displacement. Because atmospheric pressure exerts a load on both inland and coastal regions (e.g., Gladkikh et al. 2011; van Dam et al. 1994), it is necessary to distinguish the imprint of the sea level variations on seismic velocity changes from the influence of atmospheric pressure fluctuations. For both sea level and atmospheric pressure, we calculated the correlation coefficient between the data from the reference station (black circle in Fig. 3a) and those from other stations (square in Fig. 3a). Because high values of correlation coefficients indicate the time series from other stations are similar to the reference station (Fig. 3a), and the time series from all stations are similar (Additional file 1: Figs. S2a,b), we averaged the sea level and atmospheric pressure from all stations independently (Additional file 1: Figs. S2c,d). We then applied a bandpass filter and calculated the Pearson correlation coefficients between the two resulting time series. We searched for the period bands where the sea level cycle was most weakly correlated with atmospheric pressure. We

limited the search to periods between 3 years and 10 days (~0.000912–0.1 cycle/day). The 10-day limit was chosen on the basis of the 10-day stacking data of current traces (f^{cur}) used to estimate seismic velocity changes.

The correlation coefficients between sea level and atmospheric pressure is close to zero in several period ranges (Fig. 3b). We sought a period band in which the correlation coefficient was less than a threshold value of 0.1 (black crosses in Fig. 3b). This period band occupied the range of 12.5–274 days (~0.0036–0.08 cycle/day). We used this period band for filtering the time series of seismic velocity changes and sea level changes in step 2.

Step 2: Evaluating the sea level influence on seismic velocity changes

We applied a bandpass filter using the period band from step 1 to the time series of sea level and seismic velocity changes for each seismic station pair. We then calculated the absolute Pearson correlation coefficients between the filtered sea level and seismic velocity changes. We assumed the observed seismic velocity change between a pair of stations as the average velocity change at two stations (Hobiger et al. 2012; Ikeda and Tsuji 2018) because the kernel's sensitivity peak would be equally high at both stations (e.g., Pacheco and Snieder 2005, 2006). We expect the seismometer located closer to the coast would be more strongly influenced by ocean perturbations. Therefore, for each seismic station pair, we defined the distance between the coast and the seismometer that was located closest to the coast (Fig. 4a), and then used those

distances to group the station pairs with the same distance, resulting in 92 distance clusters (Fig. 4b).

Once we grouped the station pairs, we averaged the absolute correlation coefficients within each distance cluster (Fig. 5). The resulting scatterplot indicated a trend of decreasing correlations with increasing coastal distance in the time series filtered within the range of 100–274 days (Fig. 5a). At wider filtering period bands (e.g., 58–274 to 41–274 days), the decreasing trend was weaker (Figs. 5b and 5c). This finding suggests that the influence of sea level is observable only in a limited period band.

Step 3: Evaluating the significance of the decreasing trend

Under the assumption that the influence of ocean loading decreases away from the coast, we evaluated the optimum period band where the influence of sea level was strongest by testing the hypothesis of a linear relationship between the correlation coefficient and distance to the coast. We defined the dependent variable Y_i as the averaged absolute correlations and the independent variable X_i as the distance to the coast (of 92 distance bins). We evaluated the significance of the correlation between X_i and Y_i with Student's t-test, which has been used in geophysical studies (e.g., Hunt et al. 2014; Kalkomey 1997; Khandelwal 2013). The value of t is defined by

$$t\text{-value} = \left(R\sqrt{n-2}\right)/\left(\sqrt{1-R^2}\right), \quad (4)$$

where n is the number of samples, and R is the Pearson correlation coefficient. We calculated the t-value for the scatterplots in step 2, using the period bands from step 1.

We used two hypotheses in this evaluation, the null hypothesis (H_0, $R = 0$) and the alternative hypothesis (H_1, $R \neq 0$). Two types of error might occur while testing the null hypothesis: type I error, in which we incorrectly reject the null hypothesis (false positive), and type II error, in which the null hypothesis is false but we fail to reject it (false negative). The probability of making a type I error is defined as significance level α.

When testing H_1, we compared the probability value (p-value) with the significance level α to evaluate whether the correlation between X_i and Y_i was due to chance or not. The p-value of our estimated t-value in eq. 4 was obtained from the Student's *t*-distribution table.

Since we tested the evidence for $R \neq 0$, we used a double-tailed Student's *t*-distribution. If our p-value is smaller than the significance level α, the null hypothesis can be rejected. The significance level usually lies between 0 and 1, although the choice of α is arbitrary. The greater the sample size, the more likely a significant relationship will be correctly identified if one exists (Thiese et al. 2016); however, a large sample size may also cause a nonsignificant relationship to appear statistically significant (p-value < α). Hence, a low significance level, such as 0.005 or 0.001, is preferred for a large sample size (Kim and Choi 2019). With the total sample consisting of 92 distance clusters, we adopted a significance level α of 0.001.

Results

Figure 6 shows examples of scatterplots based on the period bands from step 1. Additional file 2: Table 1 shows the results for all possible period bands. The R values are mostly negative. Within the ranges of 78–274, 91–219, and 84–183 days, the p-value is smaller than 0.001. However, at wider ranges (e.g., 73–274 to 41–274 days), the correlation is weaker, and the p-value exceeds 0.001 (Fig. 6 and Additional file 2: Table 1). The period bands with high absolute R and p-value < α indicate stronger evidence of a decreasing trend. We selected 100–274 days, with the strongest correlation (R = –0.41) and the smallest p-value (0.000046), as the optimum period band (Fig. 7a).

The correlation values between sea level and seismic velocity changes are shown in Figure 8 for all seismic station pairs. Focusing on station pairs with absolute correlations > 0.2, 82 station pairs had negative correlations and 45 pairs had positive correlations between seismic velocity change and sea level (Figs. 8b and 8c, respectively). Among these more strongly correlated station pairs, those with negative correlations tended to be on the western side of the study region, and those with positive correlations slightly favored the eastern part. Figure 9 shows examples of filtered and unfiltered time series used for station pairs with negative correlations greater than 0.4, and Figure 10 shows examples of the time series for the station pairs with positive correlations greater than 0.4.

Discussion

Comparison with non-oceanic perturbations

To validate if the selected period band could represent the sea level influence on seismic velocity changes, we compared our result with those for other environmental variables. Figure 7b shows a scatterplot of atmospheric pressure versus seismic velocity changes, using the same period band. This plot displays no appreciable trend (R = 0.06), nor is the regression statistically significant (p-value = 0.5), indicating that the trend in Figure 7b unlikely reflect the perturbation from the atmospheric pressure.

We also considered whether rainfall could account for the negative trend like the one shown in Figure 7a. Rainfall requires an infiltration process to influence seismic velocity change. For periods between 100 – 274 days, the precipitation cycle at most precipitation gauges tends to be similar to the sea level cycle, especially in northern Chugoku and central Shikoku (Additional file 1: Fig. S3). This similarity makes it difficult to evaluate the possibility of an infiltration effect (Andajani et al. 2020). A comparison of total annual precipitation at each gauge and its proximity to the coast (Additional file 1: Fig. S4) shows that some stations within 20 km of the coast have higher total annual precipitation than other stations and thus could be susceptible to rainfall perturbations. However, the absence of a clear trend between total precipitation and distance from the coast means that the decreasing trend in Figure 7 is not associated with the amount of precipitation.

We also compared the magnitude of other perturbations that can influence seismic velocity changes near the coast. Changes in atmospheric pressure as large as ~10^3 Pa have been shown to cause temporal variations in seismic velocity at various depths (Silver et al. 2007, Niu et al. 2008). Assuming that the amplitudes of the Earth

tide and ocean tide are similar, the amplitude of the 0.5-year period in the study region is ~1.7 cm (Japan Coast Guard 2021), corresponding to ~170 Pa. Our calculations for the 100–274 day period band show that changes in atmospheric pressure amount to ~2 to 5×10^2 Pa, while the change in the sea level is ~3 to 15 cm (the red line in the Additional file 1: Figs. S2c and S2d) that equals ~3 to 15×10^2 Pa. These comparisons show that the magnitude of the sea-level change is larger than the contribution from atmospheric pressure variations and earth tides. Therefore, the external forcing in the period band of 100 – 274 days is likely to be dominated by the perturbation from the ocean.

Interpretation of the mechanism

The selected period range from 100 – 274 days registers the influence of sea level at the coast, which may be due to several factors such as river runoff, seasonal changes in mean sea level, and tides (Fig. 2 in Woodworth et al. 2019). Variations in sea level are known to deform the lithosphere and cause surface displacements (e.g., Neumeyer et al. 2005; van Dam et al. 1997). Ocean loading bends the land, pushing the crust downward and subjecting the upper crust to dilation. Given that seismic velocity estimated from coda waves is sensitive to external loads (e.g., Grêt et al. 2006; Wang et al. 2008), seismic velocity changes could be ascribed to inland stress changes due to sea level variation.

Adding or removing masses of water can deform the Earth's crust and cause surface displacements. For example, removing water equivalent to a layer 1 m thick in an area of 20 km radius can cause vertical and horizontal displacements for several

millimeters at sites located at tens of kilometers from the source (Fig. 1 in Wahr et al. 2013). We observed negative correlations as strong as –0.45 between sea level and seismic velocity changes around 25 km from the coast (Fig. 9c) and positive correlations as strong as ~0.4 within 15.6 km from the coast (Fig. 10d). Non-tidal ocean loading is known to influence the GPS sites within 50 km of the ocean (e.g., van Dam et al. 1997). All of the seismic stations in our study region, being less than 50 km from the coast, were considered subject to effects of ocean loading.

Vertical and horizontal deformation due to ocean loading reflect changes in vertical stress and inland bending. Geodetic studies based on GPS signals show that vertical displacements from movements of a concentrated mass (e.g., mass discharge to the ocean) tend to be larger than horizontal displacements (van Dam et al. 1997; Wahr et al. 2013). Considering this, we assumed that vertical stress change produces the dominant effect on the land by the mechanism depicted in Figure 11a: as sea level rises, the seawater mass exerts a load on the seafloor and the adjacent land area (the blue arrows) such that the upper crust shifts downward and toward the ocean (the black arrows). The combined effect of these movements causes vertical compression in the subsurface.

Possible factors that cause the variation in the seismic velocity change

Many factors can generate positive and negative correlations between seismic velocity change and sea level variability related to ocean loading (Fig. 8). Here, we consider

several possible factors that may cause such variations, for example, the *in situ* stress state, the orientation of cracks, and hydraulic conductivity.

The first possibility is that seismic velocity change reflects the stress state (i.e., effective stress and pore pressure) induced by the sea level variability. Ocean loading is known to perturb stress both offshore and onshore. Considering that the present *in situ* stress is influenced by geological features such as faults and folds, the stress conditions is likely to vary in different areas. Thus, the oceanic perturbation can cause onshore stress to increase or decrease, which can cause either a positive or negative correlation between seismic velocity change and sea level.

Next, the variation in the seismic velocity can also be influenced by the presence and the orientation of cracks. Depending on the cracks orientation, cracks can introduce seismic anisotropy. Cracks can be deformed (close or open) because of the stress induced by the ocean loading. Here, we assume that the coda signal used in estimating seismic velocity changes is dominated by the energy of surface (Rayleigh) waves (e.g., Obermann et al. 2015; Wu et al. 2016). The surface wave velocity is associated with shear wave velocity (Xia et al. 1999), which in turn is sensitive to the opening and closing of microcracks. The seismic velocity changes in our study region mostly reflect the temporal variation of S-wave velocities within the 1.5–2 km depth range (Andajani et al. 2020). It is possible to interpret seismic velocity changes in terms of the opening or closure of microcracks due to stress changes imposed by ocean loading. Suppose the vertical stress change is dominant on the land, the cracks will close if the dominant cracks are horizontal, whereas these cracks will open if they are closer to the vertical

(Fig. 11b). Thus, these crack orientations may explain both positive and negative correlations between seismic velocity and sea level.

Finally, we consider the contribution of fluid hydraulic conductivity with the change of vertical stress. Depending on lithologic conditions, the correlation between seismic velocity change and sea level change may be positive or negative. For example, in relatively impermeable rocks, the increase of vertical compression can increase pore pressure to the point of generating cracks (white arrows in Fig. 11c). This reduces the seismic velocity, resulting in a negative correlation between seismic velocity change and sea level. The vertical stress change can also increase the rock's effective stress if the pore pressure is negative or fluid flows out in highly permeable rocks. This causes the seismic velocity to increase. This results in a positive correlation between seismic velocity change and sea level change.

We concluded that temporal changes in seismic velocity could be dominated by external perturbations, including sea level variability. Our analysis suggests that the crust closer to the coast can be susceptible to the ocean loading. The absolute correlation between seismic velocity change and sea level change decreased with increasing seismic station distance from the coast. Ocean loading marked by sea level increase caused the land local stress to change. In situ stress condition, fracture orientation, and fluid role likely contribute to the seismic velocity change. Note that this study is still an exploratory work as our interpretation is based on a simple model that ignores many tidal and non-tidal factors and steric effects that affect sea level. To better evaluate the stress change at coastal areas related to the sea level increase, further

analysis should be carried out by comparing the seismic velocity monitoring with a quantitative model of the ocean mass redistribution around the Chugoku Shikoku regions.

Conclusion

In this study, we analyzed temporal changes in seismic velocity from ambient noise to evaluate the imprint of temporal changes in crustal conditions related to environmental loading on observed changes in shear velocity. Our results support the hypothesis that seismic velocity changes in coastal regions are affected by variations in sea level. By taking into account the station's proximity to the coast, we were able to emphasize the imprint of sea level in seismic velocity changes. A statistical analysis revealed that the absolute correlation between ocean perturbation and seismic velocity tends to decrease with increasing distance from the coast. We show that consideration of station's distance from the coast helps to distinguish the influence of sea level on seismic velocity monitoring. Our primary conclusions are:

(1) Variations in sea level may influence seismic velocity changes through the shallow crustal deformation induced by ocean loading. This is consistent with the decreasing strength of the absolute correlation between sea level and seismic velocity change with increasing distance from the coast.

(2) The imprint of sea-level variability on seismic velocity changes persists at least up to dozens of kilometers inland from the coast.

(3) The increase of sea level deforms the ocean bottom and causes the land to experience vertical compression in the subsurface. The resulting inland local stress changes influence seismic velocity changes.

(4) Depending on the inland crack's orientation, the correlation between seismic velocity change and sea level can be either negative or positive. With the dominant vertical stress change, if the dominant cracks are perpendicular to the vertical stress, the cracks will open as sea level increases (negative correlation with sea level). On the other hand, if the dominant cracks are parallel to the vertical stress, the cracks will close (positive correlation with sea level).

(5) Lithology condition contributes to the correlation between seismic velocity change and sea level. A positive correlation may reflect cracks closure related to increased effective stress caused by negative pore pressure or fluid loss in highly permeable rock as the subsurface is vertically compressed. Meanwhile, a negative correlation implies cracks generation because of increased pore pressure in low permeability rocks.

Figure Legends

Fig. 1. a Location map of Japan showing the study area in the Chugoku and Shikoku regions, **b** bedrock map of the study region (modified from the Geological Survey of

Japan AIST, 2015), and location maps of **c** seismic stations, **d** atmospheric pressure gauges, and **e** ocean tidal observations

Fig. 2. Flowchart summarizing the workflow of this study

Fig. 3. a Maps of the study region showing the similarity of each station time series to that of the reference station for sea level (left panel) and atmospheric pressure (right panel). **b** Plot showing Pearson correlation coefficients between sea level and atmospheric pressure for various period bands (step 1). The black crosses indicate the range of period bands in which the absolute correlation coefficient between sea level and atmospheric pressure is less than 0.1. The period displays within 20 – 1096 period band.

Fig. 4. a Schematic diagram showing the definition of distance to the coast for seismic station pairs. **b** Histogram showing the number of seismic station pairs in each distance cluster

Fig. 5. Scatterplots between the average absolute correlation between sea level and seismic velocity change and the distance from the coast for period bands of **a** 100–274, **b** 58–274, and **c** 41–274 days

Fig. 6. a Correlation values and **b** *p*-values for a range of period bands listed in Additional file 2: Table 1. In panel **a,** the period displays within 41 -274 period band. In **b**, only *p*-values less than 0.001 are shown

Fig. 7. Scatterplots from step 2 plotting distance from the coast against the correlations between **a** seismic velocity changes and sea level data and **b** seismic velocity changes and atmospheric pressure after filtering within the 100–274 day period band

Fig. 8. Maps of the study region showing correlations between seismic velocity change and sea level for **a** all seismic station pairs, **b** station pairs with negative correlations stronger than –0.2, and **c** station pairs with positive correlations stronger than 0.2. Seismic velocity changes and sea level data are filtered within the 100–274 day period band

Fig. 9. Examples of time series of seismic velocity change (blue) and sea level (black) for station pairs (a–d) with negative correlations

Fig. 10. Examples of time series of seismic velocity change (blue) and sea level (black) for station pairs (a–d) with positive correlations

Fig. 11. a Schematic diagram illustrating the inland surface displacement associated with ocean loading and inferred effects on seismic velocity. Increasing sea water mass exerts a load on the seafloor and the nearby coast (blue arrows), resulting in vertical and

horizontal displacements of the land (black arrows). The dominant vertical displacement causes compression in the subsurface that can result in possible outcomes: **b** change of cracks (marked by the black arrow) and **c** change of pore pressure conditions(pore pressure increase is marked by the white arrow) that affect the response of seismic velocity to ocean loading.

Declarations

Availability of data and materials

Seismic data required to evaluate the conclusions in the paper are available from NIED (http://www.hinet.bosai.go.jp/about_data/?LANG=en). The meteorological data were obtained from JMA (https://www.jma.go.jp/jma/index.html)

Authors' contributions

RDA proposed this study and drafted the initial manuscript. TT, RS, and TI suggested the method for the interpretation, and revised the manuscript. All authors read and approved the final manuscript.

Competing interests

The authors declare that they have no competing interests.

Funding

This work was supported by Japan Society for the Promotion of Science grants (no. JP20H01997).

Acknowledgments

We used Hi-net seismic data from the National Research Institute for Earth Science and Disaster Resilience (NIED). We obtained rainfall, sea level, and atmospheric pressure data from the Japan Meteorological Agency (JMA). We appreciate Fernando Lawrens Hutapea (Kyushu Univ.) for his technical support in computing seismic velocity change. This study was also supported by Japan Society for the Promotion of Science grants (no. JP20H01997). We are grateful for the support provided by the Advanced Graduate Program in Global Strategy for Green Asia of Kyushu University, and International Institute for Carbon-Neutral Energy Research (I2CNER) funded by the World Premier International Research Center Initiative of the Ministry of Education, Culture, Sports, Science and Technology, Japan (MEXT).

References

Albino F, Pinel V, Sigmundsson F (2010) Influence of surface load variations on eruption likelihood: application to two Icelandic subglacial volcanoes, Grímsvötn and Katla. Geophys J Int 181(3): 1510 - 1524. https://doi.org/10.1111/j.1365-246X.2010.04603.x

Andajani RD, Tsuji T, Snieder R, Ikeda T (2020) Spatial and temporal influence of rainfall on crustal pore pressure based on seismic velocity monitoring. Earth, Planets Sp 72(1):117. https://doi.org/10.1186/s40623-020-01311-1

Donaldson C, Winder T, Caudron C, White RS (2019) Crustal seismic velocity responds to a magmatic intrusion and seasonal loading in Iceland ’s Northern Volcanic Zone. Sci Adv 5(11):eaax6642. https://doi.org/10.1126/sciadv.aax6642

Geological Survey of Japan, AIST (ed.) (2015) Seamless digital geological map of Japan 1:200,000. May 29, 2015 version. Geological Survey of Japan, National Institute of Advanced Industrial Science and Technology. https://gbank.gsj.jp/geonavi/. Accessed 10 Feb 2021.

Gladkikh V, Tenzer R, Denys P (2011) Crustal Deformation due to Atmospheric Pressure Loading in New Zealand. J Geod Sci. 1(3):271–279. https://doi.org/10.2478/v10156-011-0005-z

Grêt A, Snieder R, Scales J (2006) Time-lapse monitoring of rock properties with coda wave interferometry. J Geophys Res Solid Earth 111(B3). https://doi.org/10.1029/2004JB003354

Hadziioannou C, Larose E, Coutant O, Roux P, Campillo M (2009) Stability of monitoring weak changes in multiply scattering media with ambient noise correlation: Laboratory experiments. J Acoust Soc Am 125(6):3688-3695. https://doi.org/10.1121/1.3125345

Haigh ID (2017) Tides and Water Levels. In: Carlton J, Jukes P, Choo YS (eds) Encyclopedia

of Maritime and Offshore Engineering. John Wiley & Sons, Ltd, Chichester, UK, pp 1–13. https://doi.org/10.1002/9781118476406.emoe122

Hatanaka Y, Sengoku A, Sato T, et al (2001) Detection of Tidal Loading Signals from GPS Permanent Array of GSI Japan. J Geod Soc Japan 47(1): 187-192. https://doi.org/10.11366/sokuchi1954.47.187

Hillers G, Ben-Zion Y, Campillo M, Zigone D (2015) Seasonal variations of seismic velocities in the San Jacinto fault area observed with ambient seismic noise. Geophys J Int. 202(2):920–932. https://doi.org/10.1093/gji/ggv151

Hobiger M, Wegler U, Shiomi K, Nakahara H (2012) Coseismic and postseismic elastic wave velocity variations caused by the 2008 Iwate-Miyagi Nairiku earthquake, Japan. J Geophys Res Solid Earth 117(B9). https://doi.org/10.1029/2012JB009402

Hunt L, Hadley S, Reynolds S, et al (2014) Precise 3D seismic steering and production rates in the Wilrich tight gas sands of West Central Alberta. Interpretation 2(2):SC1–SC18. https://doi.org/10.1190/INT-2013-0086.1

Hutapea FL, Tsuji T, Ikeda T (2020) Real-time crustal monitoring system of Japanese Islands based on spatio-temporal seismic velocity variation. Earth, Planets Sp 72(1):19. https://doi.org/10.1186/s40623-020-1147-y

Ikeda T, Tsuji T (2018) Temporal change in seismic velocity associated with an offshore MW 5.9 Off-Mie earthquake in the Nankai subduction zone from ambient noise cross-correlation. Prog Earth Planet Sci 5(1):62. https://doi.org/10.1186/s40645-018-0211-8

Japan Coast Guard (JCG) (2021) Hydrographic and Oceanographic Department. https://www1.kaiho.mlit.go.jp/TIDE/gauge/index_eng.php. Accessed 10 Feb 2021.

Kalkomey CT (1997) Potential risks when using seismic attributes as predictors of reservoir properties. Lead Edge 16(3):247–251. https://doi.org/10.1190/1.1437610

Khandelwal M (2013) Correlating P-wave Velocity with the physico-mechanical properties of different rocks. Pure Appl Geophys 170(4):507–514. https://doi.org/10.1007/s00024-012-0556-7

Kim JH, Choi I (2019) Choosing the Level of Significance: A Decision-theoretic Approach. Abacus 57(1): 27-71. https://doi.org/10.1111/abac.12172

Matthews AJ, Barclay J, Johnstone JE (2009) The fast response of volcano-seismic activity to intense precipitation: triggering of primary volcanic activity by rainfall at Soufrière Hills Volcano, Montserrat. J Volcanol Geotherm Res 184(3):405–415. https://doi.org/10.1016/j.jvolgeores.2009.05.010

Minato S, Tsuji T, Ohmi S, Matsuoka T (2012) Monitoring seismic velocity change caused by the 2011 Tohoku-oki earthquake using ambient noise records. Geophys Res Lett 39(9). https://doi.org/10.1029/2012GL051405

Mordret A, Mikesell TD, Harig C, et al (2016) Monitoring southwest Greenland ’s ice sheet melt with ambient seismic noise. Sci Adv 2(5):e1501538. https://doi.org/10.1126/sciadv.1501538

Nakata N, Snieder R (2012) Estimating near-surface shear wave velocities in Japan by applying seismic interferometry to KiK-net data. J Geophys Res Solid Earth 117(B1). https://doi.org/10.1029/2011JB008595

Neuberg J (2000) External modulation of volcanic activity. Geophys J Int 142(1):232–240. https://doi.org/10.1046/j.1365-246X.2000.00161.x

Neumeyer J, del Pino J, Dierks O, et al (2005) Improvement of ocean loading correction on gravity data with additional tide gauge measurements. J Geodyn 40(1):104–111 https://doi.org/10.1016/j.jog.2005.07.012

Nimiya H, Ikeda T, Tsuji T (2017) Spatial and temporal seismic velocity changes on Kyushu Island during the 2016 Kumamoto earthquake. Sci Adv 3(11):e1700813. https://doi.org/10.1126/sciadv.1700813

Niu F, Silver PG, Daley TM, et al (2008) Preseismic velocity changes observed from active source monitoring at the Parkfield SAFOD drill site. Nature 454(7201):204–208. https://doi.org/10.1038/nature07111

Obara K, Kasahara K, Hori S, Okada Y (2005) A densely distributed high-sensitivity seismograph network in Japan:Hi-net by National Research Institute for Earth Science and DisasterPrevention. Rev Sci Instrum 76(2):21301. https://doi.org/10.1063/1.1854197

Obermann A, Kraft T, Larose E, Wiemer S (2015) Potential of ambient seismic noise techniques tomonitor the St. Gallen geothermal site (Switzerland). J Geophys Res Solid Earth 120(6):4301–4316. https://doi.org/10.1002/2014JB011817

Pacheco C, Snieder R (2005) Time-lapse travel time change of multiply scattered acoustic waves. J Acoust Soc Am 118(3):1300–1310. https://doi.org/10.1121/1.2000827

Pacheco C, Snieder R (2006) Time-lapse traveltime change of singly scattered acoustic waves. Geophys J Int 165(2):485–500. https://doi.org/10.1111/j.1365-246X.2006.02856.x

Richter T, Sens-Schönfelder C, Kind R, Asch G (2014) Comprehensive observation and modeling of earthquake and temperature-related seismic velocity changes in northern Chile with passive image interferometry. J Geophys Res Solid Earth 119(6):4747–4765. https://doi.org/10.1002/2013JB010695

Rivet D, Brenguier F, Clarke D, et al (2014) Long-term dynamics of Piton de la Fournaise volcano from 13 years of seismic velocity change measurements and GPS observations. J Geophys Res Solid Earth 119(10):7654–7666. https://doi.org/10.1002/2014JB011307

Sato T, Fukuda Y, Aoyama Y, et al (2001) On the observed annual gravity variation and the effect of sea surface height variations. Phys Earth Planet Inter 123(1):45–63. https://doi.org/10.1016/S0031-9201(00)00216-8

Sens-Schönfelder C, Wegler U (2006) Passive image interferemetry and seasonal variations of seismic velocities at Merapi Volcano, Indonesia. Geophys Res Lett 33(21). https://doi.org/10.1029/2006GL027797

Silver PG, Daley TM, Niu F, Majer EL (2007) Active source monitoring of cross-well

seismic travel time for stress-induced changes. Bull Seismol Soc Am 97(1B):281–293. https://doi.org/10.1785/0120060120

Takano T, Nishimura T, Nakahara H (2017) Seismic velocity changes concentrated at the shallow structure as inferred from correlation analyses of ambient noise during volcano deformation at Izu-Oshima, Japan. J Geophys Res Solid Earth 122(8):6721–6736. https://doi.org/10.1002/2017JB014340

Thiese MS, Ronna B, Ott U (2016) P value interpretations and considerations. J Thorac Dis 8(9):E928-E931. https://doi.org/10.21037/jtd.2016.08.16

van Dam TM, Blewitt G, Heflin MB (1994) Atmospheric pressure loading effects on global positioning system coordinate determinations. J Geophys Res 99(B12):23939–23950. https://doi.org/10.1029/94jb02122

van Dam TM, Wahr J, Chao Y, Leuliette E (1997) Predictions of crustal deformation and of geoid and sea-level variability caused by oceanic and atmospheric loading. Geophys J Int 129(3):507–517. https://doi.org/10.1111/j.1365-246X.1997.tb04490.x

Wahr J, Khan SA, Van Dam T, et al (2013) The use of GPS horizontals for loading studies, with applications to northern California and southeast Greenland. J Geophys Res Solid Earth 118(4):1795–1806. https://doi.org/10.1002/jgrb.50104

Wang B, Zhu P, Chen Y, et al (2008) Continuous subsurface velocity measurement with coda wave interferometry. J Geophys Res Solid Earth 13(B12). https://doi.org/10.1029/2007JB005023

Wang Q-Y, Brenguier F, Campillo M, et al (2017) Seasonal Crustal Seismic Velocity Changes Throughout Japan. J Geophys Res Solid Earth 122(10):7987–8002. https://doi.org/10.1002/2017JB014307

Woodworth PL, Melet A, Marcos M, et al (2019) Forcing Factors Affecting Sea Level Changes at the Coast. Surv Geophys 40(6):1351–1397. https://doi.org/10.1007/s10712-019-09531-1

Wu C, Delorey A, Brenguier F, et al (2016) Constraining depth range of S wave velocity decrease after large earthquakes near Parkfield, California. Geophys Res Lett 43(12):6129–6136. https://doi.org/10.1002/2016GL069145

Xia J, Miller RD, Park CB (1999) Estimation of near-surface shear-wave velocity by inversion of Rayleigh waves. Geophysics 64(3):691–700. https://doi.org/10.1190/1.1444578

Figures

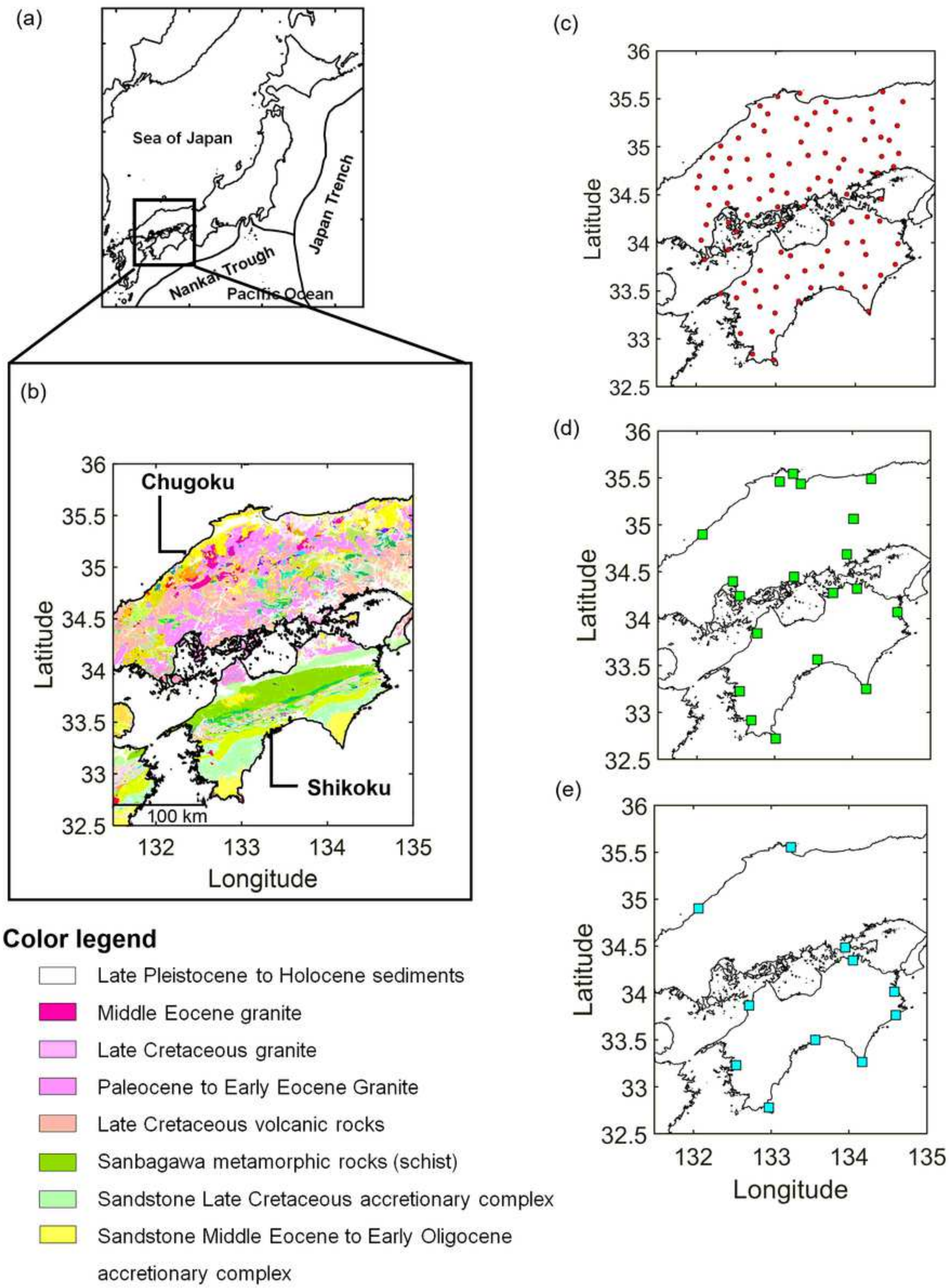

Figure 1

a Location map of Japan showing the study area in the Chugoku and Shikoku regions, b bedrock map of the study region (modified from the Geological Survey of Japan AIST, 2015), and location maps of c seismic stations, d atmospheric pressure gauges, and e ocean tidal observations

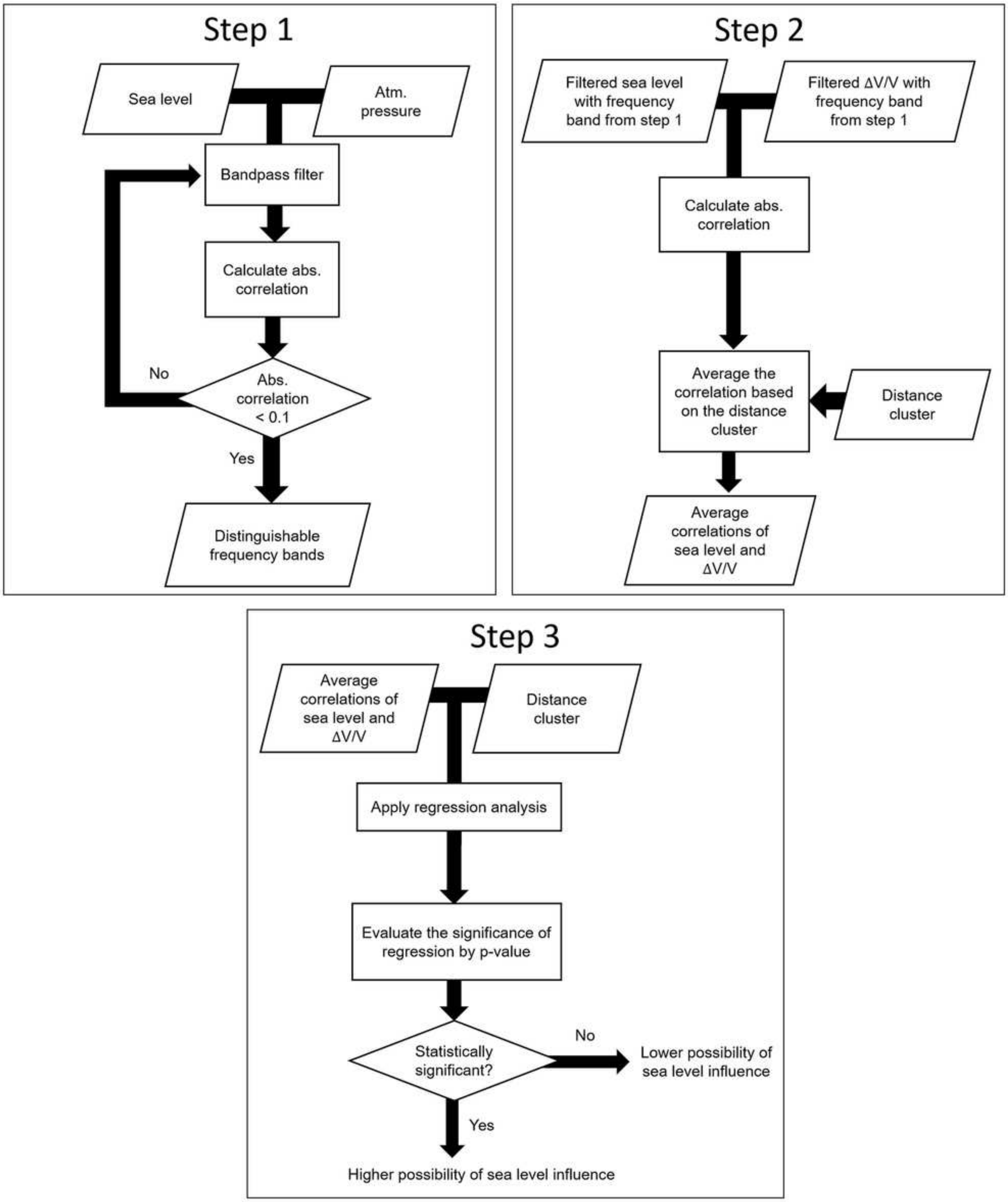

Figure 2

Flowchart summarizing the workflow of this study

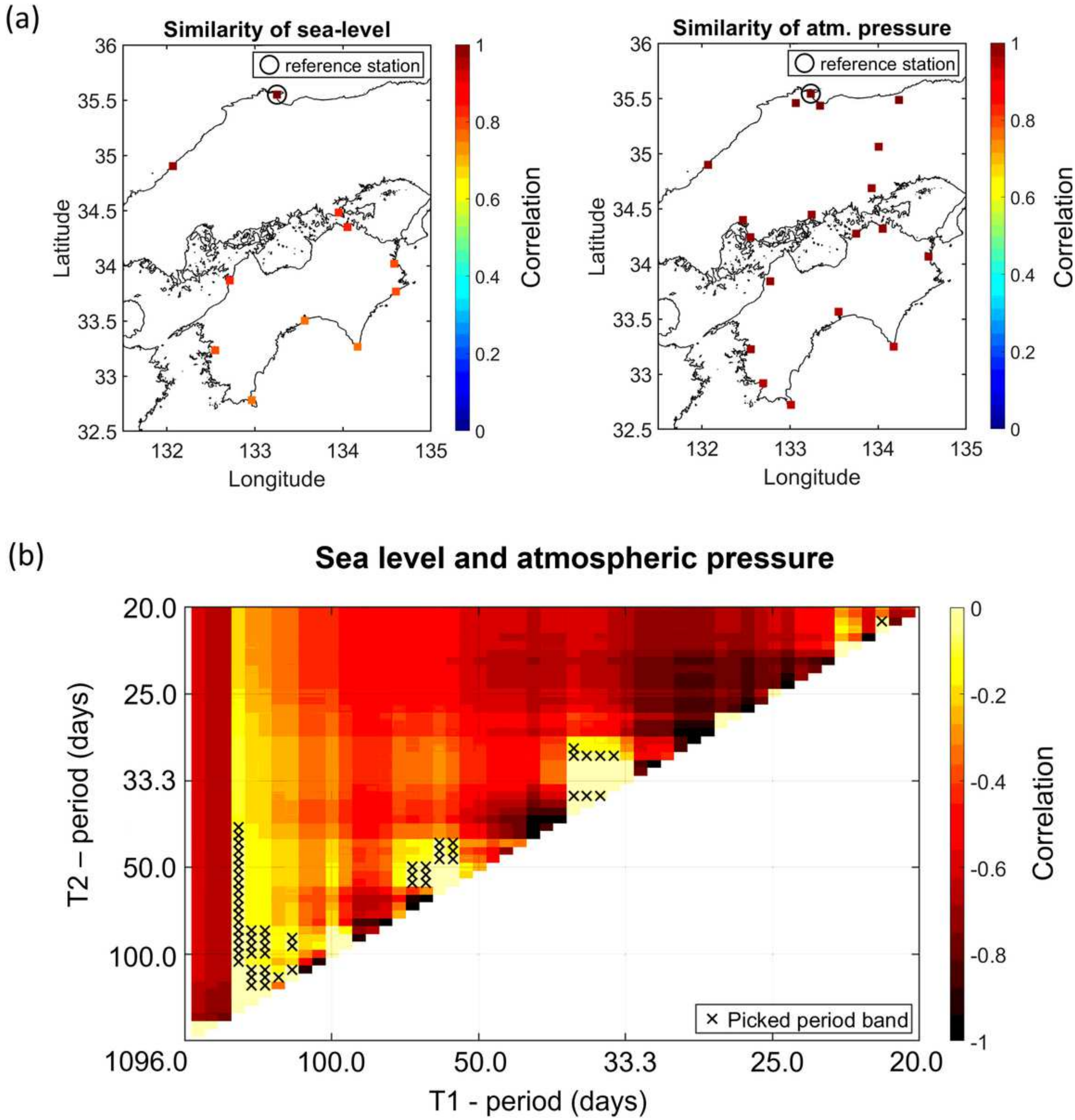

Figure 3

a Maps of the study region showing the similarity of each station time series to that of the reference station for sea level (left panel) and atmospheric pressure (right panel). b Plot showing Pearson correlation coefficients between sea level and atmospheric pressure for various period bands (step 1). The black crosses indicate the range of period bands in which the absolute correlation coefficient

between sea level and atmospheric pressure is less than 0.1. The period displays within 20 – 1096 period band.

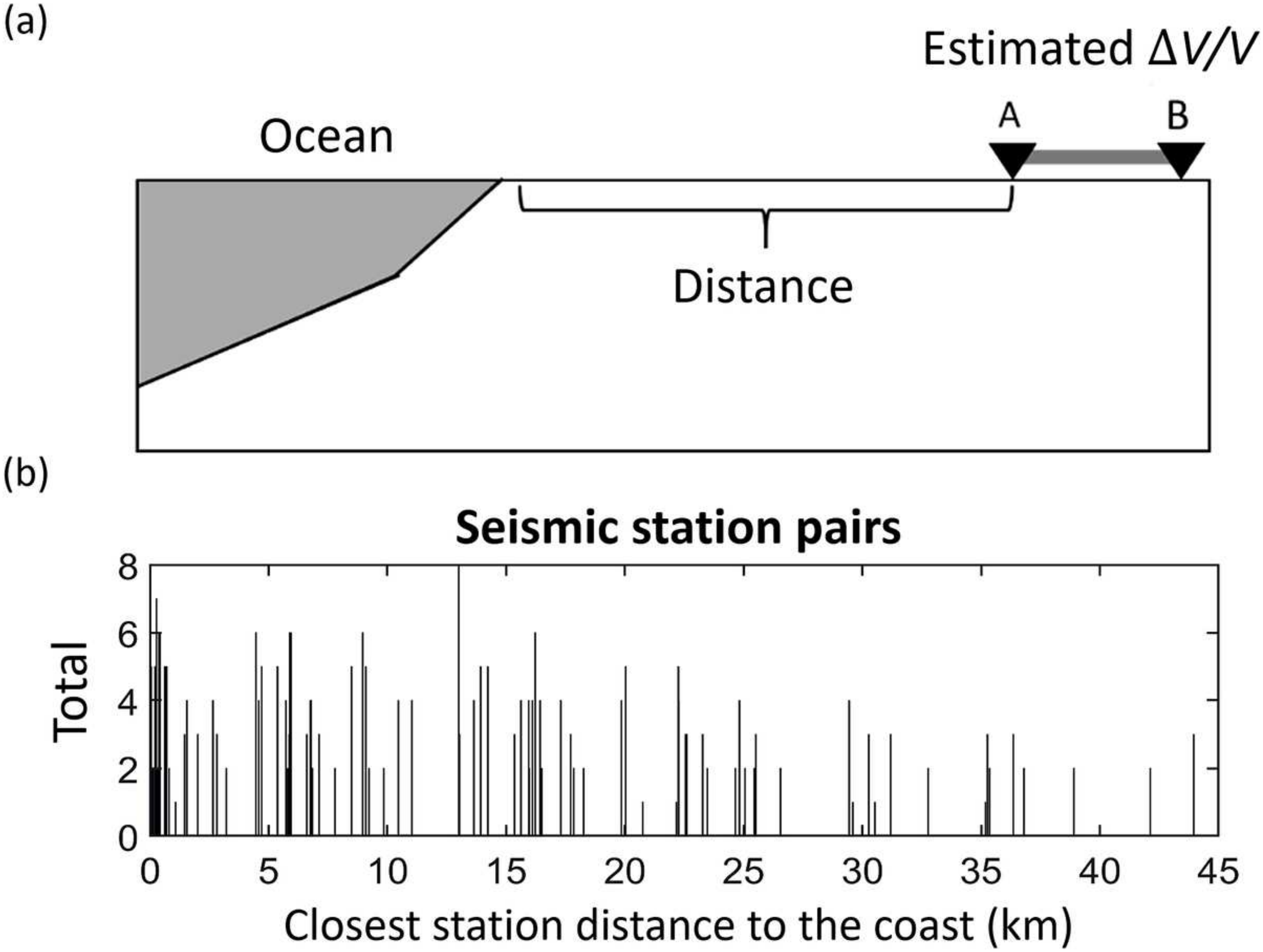

Figure 4

a Schematic diagram showing the definition of distance to the coast for seismic station pairs. b Histogram showing the number of seismic station pairs in each distance cluster

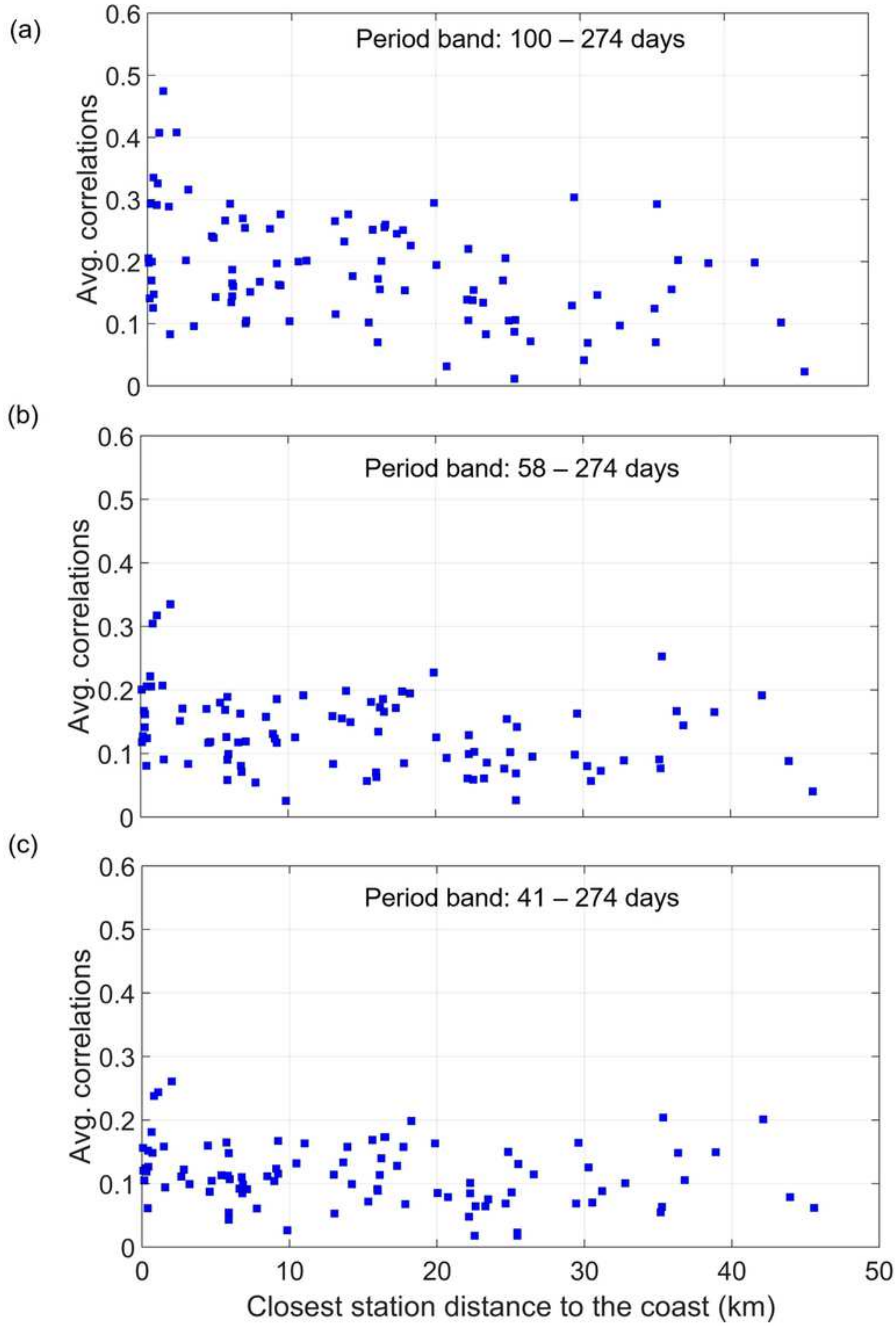

Figure 5

Scatterplots between the average absolute correlation between sea level and seismic velocity change and the distance from the coast for period bands of a 100–274, b 58–274, and c 41–274 days

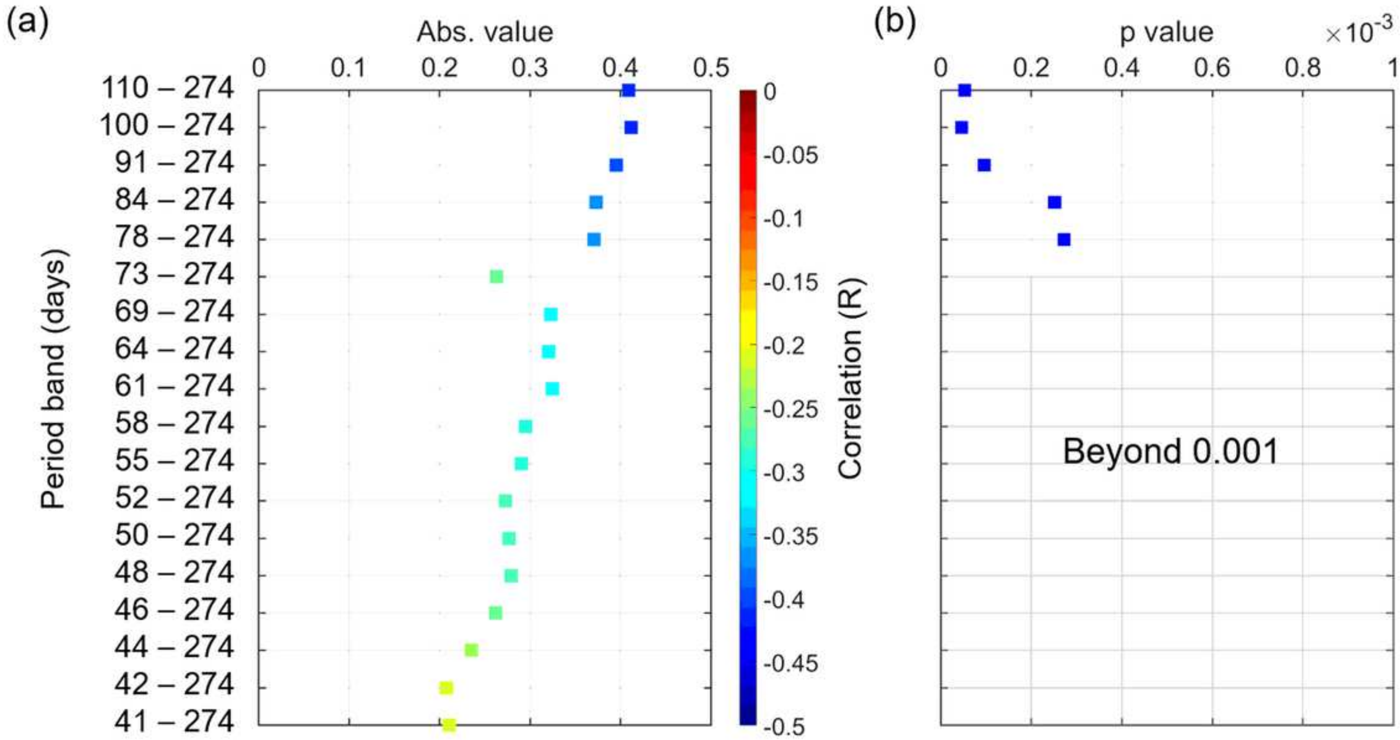

Figure 6

a Correlation values and b p-values for a range of period bands listed in Additional file 2: Table 1. In panel a, the period displays within 41 -274 period band. In b, only p-values less than 0.001 are shown

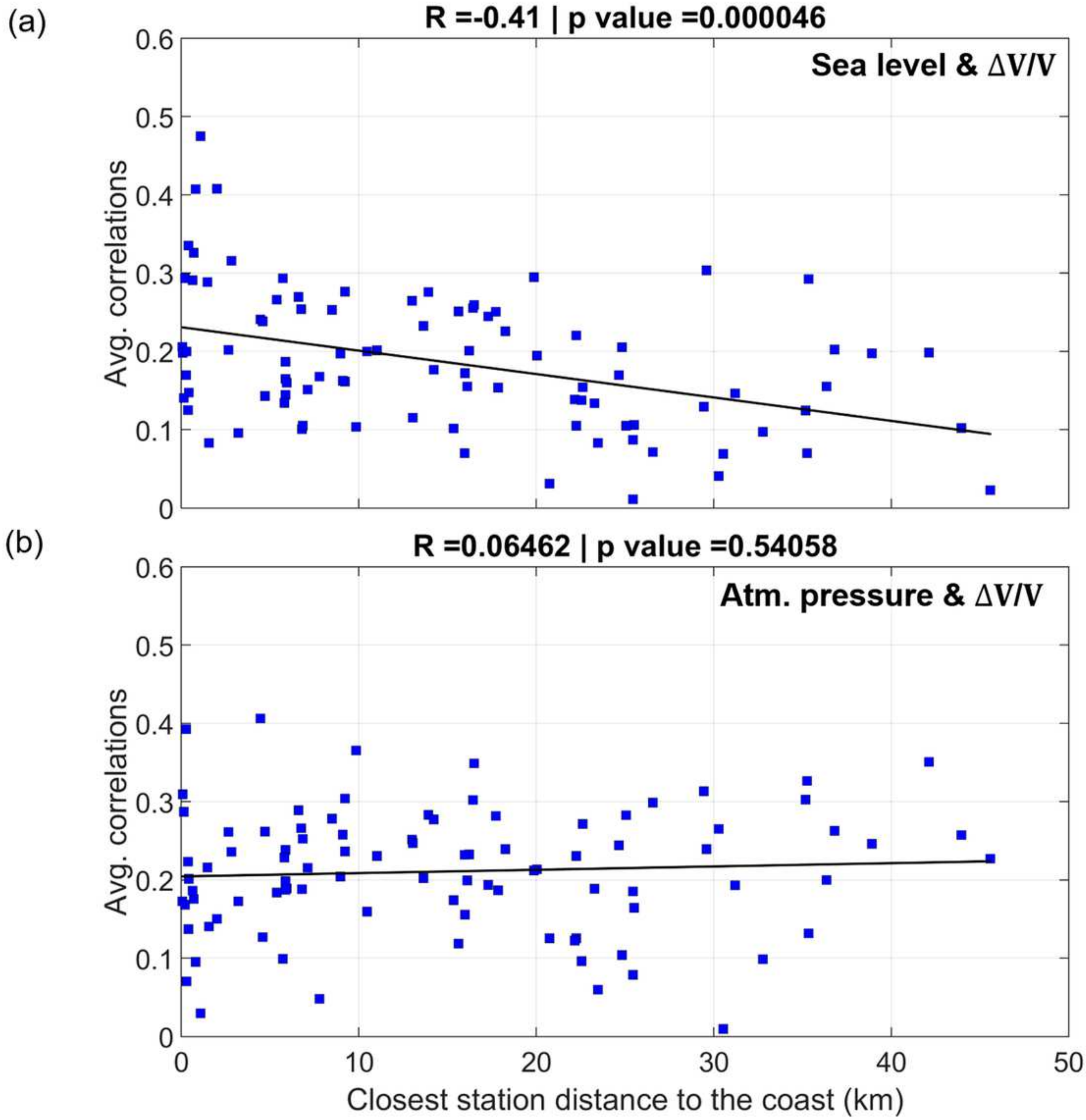

Figure 7

Scatterplots from step 2 plotting distance from the coast against the correlations between a seismic velocity changes and sea level data and b seismic velocity changes and atmospheric pressure after filtering within the 100–274 day period band

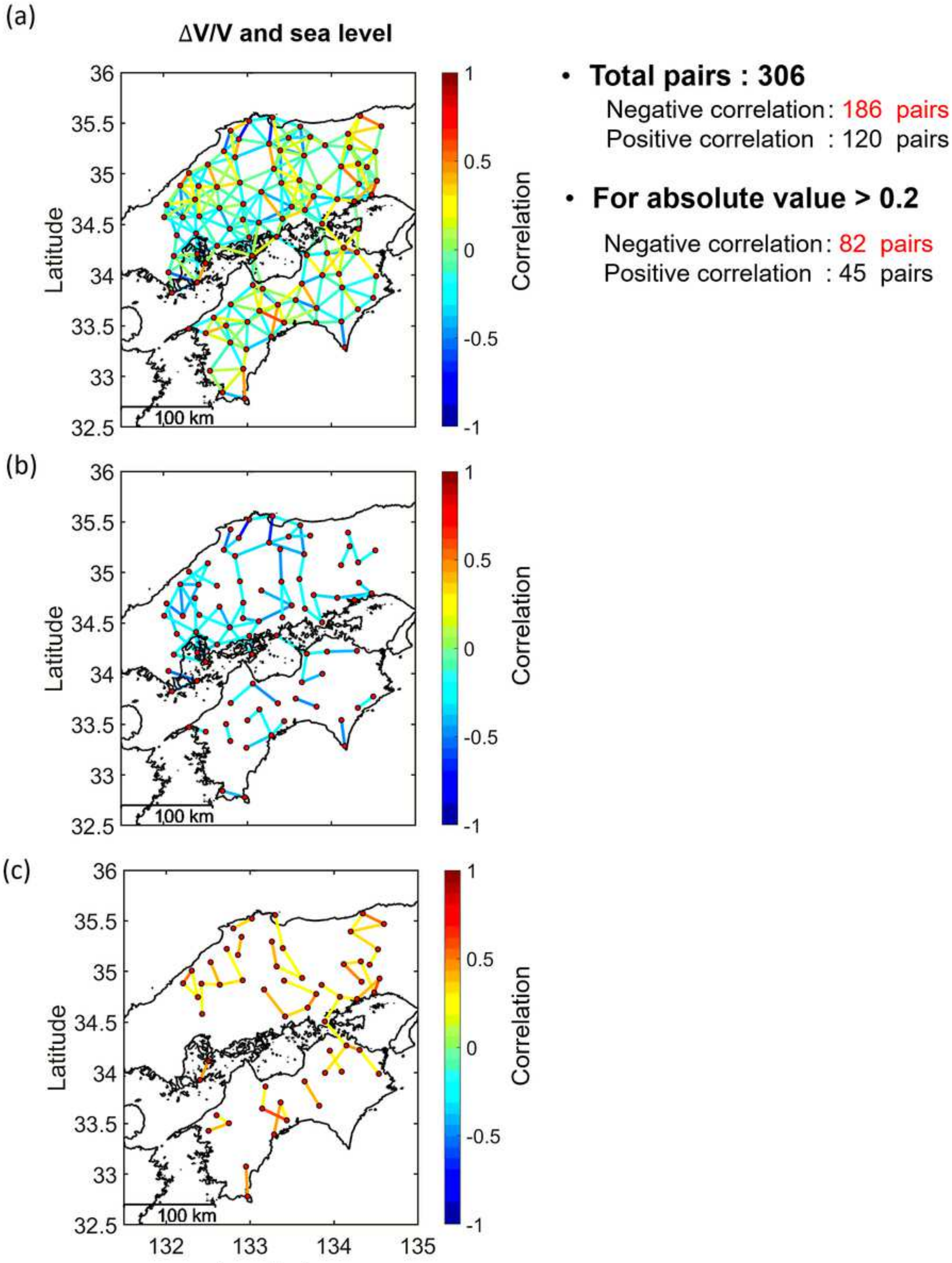

Figure 8

Maps of the study region showing correlations between seismic velocity change and sea level for a all seismic station pairs, b station pairs with negative correlations stronger than −0.2, and c station pairs with positive correlations stronger than 0.2. Seismic velocity changes and sea level data are filtered within the 100–274 day period band

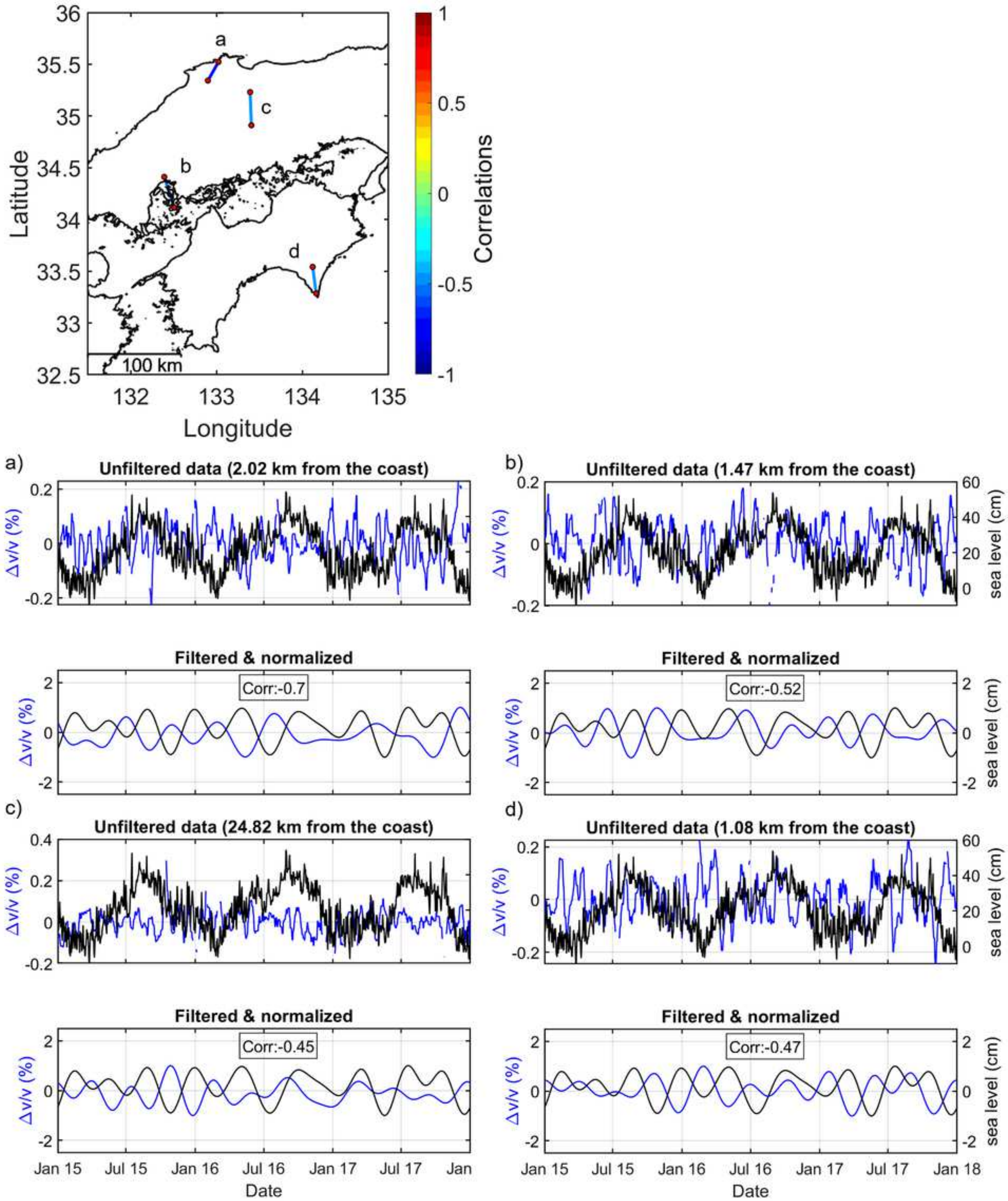

Figure 9

Examples of time series of seismic velocity change (blue) and sea level (black) for station pairs (a–d) with negative correlations

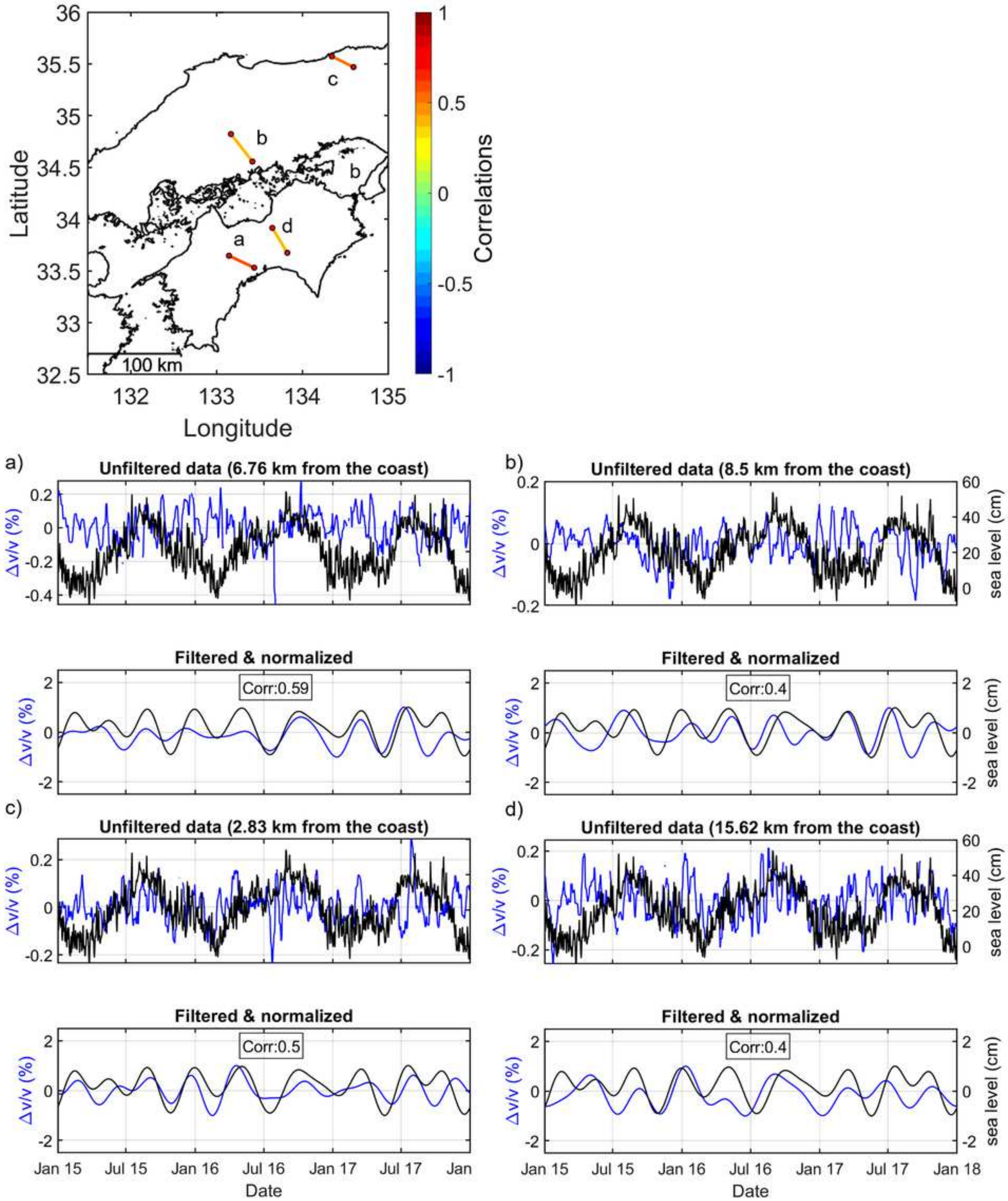

Figure 10

Examples of time series of seismic velocity change (blue) and sea level (black) for station pairs (a–d) with positive correlations

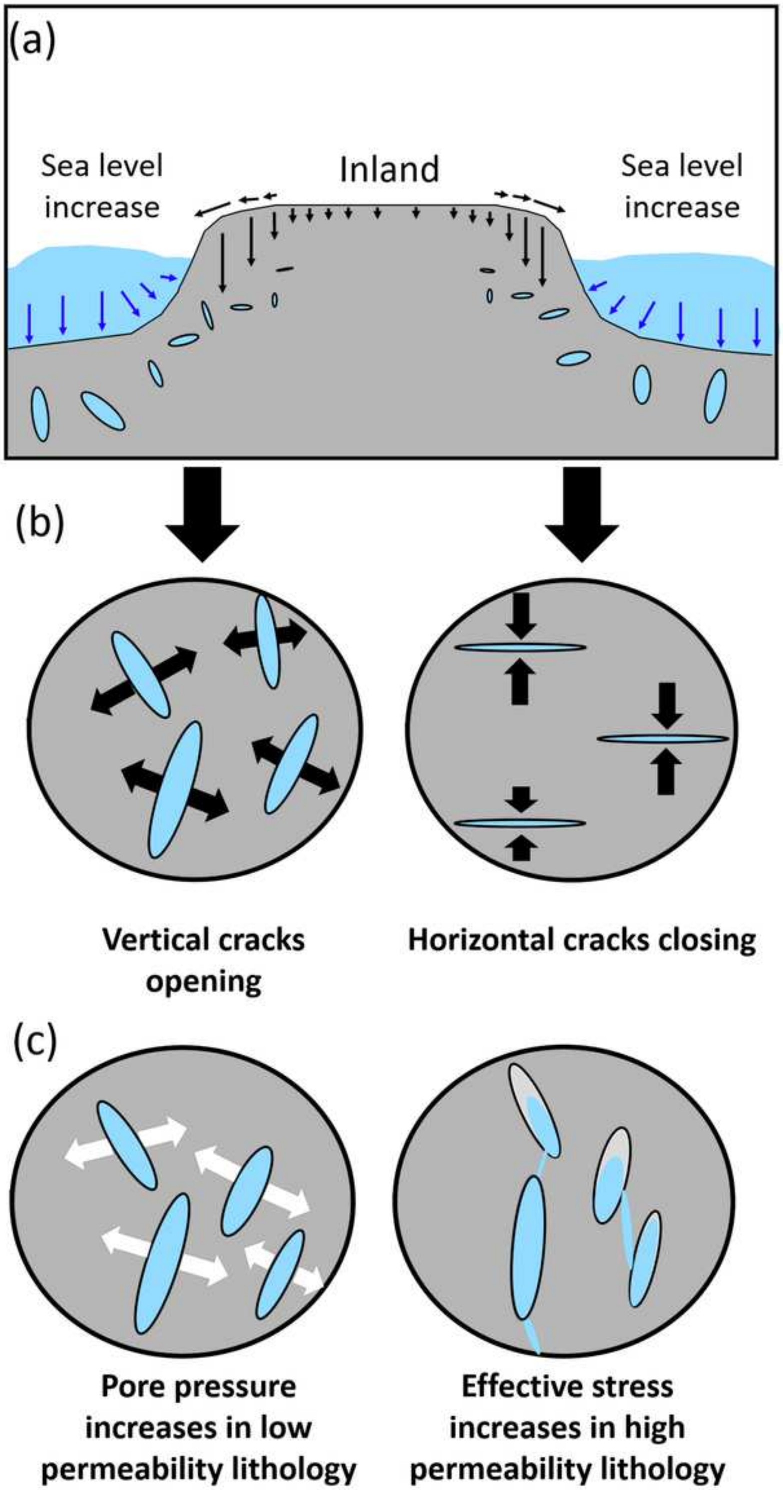

Figure 11

a Schematic diagram illustrating the inland surface displacement associated with ocean loading and inferred effects on seismic velocity. Increasing sea water mass exerts a load on the seafloor and the nearby coast (blue arrows), resulting in vertical and horizontal displacements of the land (black arrows). The dominant vertical displacement causes compression in the subsurface that can result in possible outcomes: b change of cracks (marked by the black arrow) and c change of pore pressure

conditions(pore pressure increase is marked by the white arrow) that affect the response of seismic velocity to ocean loading.

Supplementary Files

This is a list of supplementary files associated with this preprint. Click to download.

- EPSAdditionalfile1FigS1S4.pdf
- EPSAdditionalfile2Table1.csv
- GraphicalAbstract.jpg